

STUDIES AND OBSERVATIONS OF BEAM DYNAMICS NEAR A SUM RESONANCE

G. Franchetti, GSI, Darmstadt, Germany

S. Gilardoni, A. Huschauer, F. Schmidt, R. Wasef, CERN Geneva, Switzerland

Abstract

The effect of space charge on bunches stored for long term in a synchrotron can be severe for beam survival. This may be the case in projects as SIS100 at GSI or LIU at CERN. In the past decade systematic simulation studies and experiments performed at CERN and GSI have highlighted the space charge induced periodic crossing of one dimensional resonances as an underlying mechanism of long term beam loss or emittance growth. However only in 2012, for the first time, the effect of space charge on a normal third order coupled resonance was investigated at the CERN-PS. The experimental results have highlighted an unprecedented asymmetric beam response where in the vertical plane the beam exhibits a thick halo, whereas the horizontal profile has only core growth. The quest for explaining these results requires a journey through the 4 dimensional dynamics of the coupled resonance investigating the fixed-lines, and requires a detailed code-experiment benchmarking also including beam profile benchmarking. This study shows that the experimental results of the 2012 PS measurements can be explained by the dynamics of the fixed-lines with space charge also including the effect of the chromaticity.

THE ACCELERATOR CASE

Space charge effects on beam circulating in a synchrotron becomes stronger for an increased beam intensity, and the problems arising with the increased intensity define an intensity limit of performance. The space charge limit is a figure of merit used to characterize the maximum intensity tolerated by a machine. It is usually defined with respect to the beam loss, although other criteria can be used to define the limit performance: for example, emittance growth, halo formation.

For projects the space charge limit plays a significant role, because it defines the ultimate accelerator performance in terms of stored particles. Usually the space charge limit is defined by a constraint on the maximum allowed incoherent space charge tune-shift. This is dictated by the working point the machine for avoiding the overlapping of the space charge tune-spread with machine resonances. For a well placed machine working point, the maximum allowed incoherent tune-shift is usually $\Delta Q_{sc} \sim -0.25$ to avoid second, third, and fourth order resonances. Clearly this argument mainly depends on which machine resonances are significant for beam loss. If the 3rd and 4th order resonances are very weak one can use more optimistically relax the constraint to $\Delta Q_{sc} \sim -0.5$. The assessment of the real effect of the space charge on machine resonances requires a detailed study of the dynamics, and it is strongly related to the storage time.

The investigation of the effect of space charge for long term storage of a bunched beam has been motivated from the planned operations with U^{28+} ions in the SIS100 synchrotron of the FAIR project [1]. In this scenario SIS18 will operate with harmonics 2, and 4 cycles will be injected into SIS100 for a total of 8 bunches transferred in 10 buckets. An amount of 6×10^{11} ions will be accumulated during 1 second at the injection energy of 200 MeV/u. This means that the first 2 bunches from the SIS18 cycle injected into SIS100 will be stored for 1 second, namely for 1.5×10^5 turns. During this time the beam with transverse rms emittances of $\epsilon_{x,rms} = 8.75$ mm-mrad, $\epsilon_{y,rms} = 3$ mm-mrad, will be bunched with bunching factor $B_f = 0.33$, generating an incoherent space charge tune-shift of $\Delta Q_x \approx -0.2$, $\Delta Q_y \approx -0.33$. In the SIS100 RF buckets U^{28+} ions follow a longitudinal dynamics with a synchrotron tune of $Q_s \sim 4.27 \times 10^{-3}$, and over 1 second storage, a particle will perform 643 or less synchrotron oscillations. This accelerator regime is very unique with no established operational experience in the accelerator community.

The synchrotron motion pushes periodically bunched particles from regions of small transverse space charge, to the region of large space charge tune-shift (at $z = 0$). Therefore, according to the initial condition, a particle may cross a machine resonance each quarter of a synchrotron oscillation.

A fast single crossing of a weak resonance typically produces a small emittance growth: in SIS100 for U^{28+} ions a quarter of synchrotron oscillation happens in ~ 58 turns. However, over one second storage the number of resonance crossings becomes as high as ~ 2700 . The integrated effect arising from this large number of repeated resonance crossing may create a large impact generating a beam diffusion to large transverse amplitudes, hence may lead to a steady beam loss throughout the storage time. Note that for this effect to be significant requires many resonance crossings, hence it disappears, or becomes insignificant for short term storage.

The assessment of the beam dynamics in this regime is challenging. The simulations are difficult: standard PIC codes are subjected to artificial noise, which affects the long term result of the simulations [2–5]. In order to mitigate this artifact one should use a very large number of macroparticles [5], which makes unfeasible systematic studies to understand the properties of the dynamics. Especially it is difficult to develop tools which may be used to predict the effects, or to develop a theory that may allow to assess how the different beam and machine features influence the emittance growth.

SPACE CHARGE AND ONE DIMENSIONAL RESONANCES

In the past decade, the interplay of space charge and machine nonlinearities has been studied for 1D resonances, i.e. type $n_x Q_x = N$. Experimental and numerical studies on beam survival and emittance growth in this regime have been carried out in the CERN-PS in the year 2003 for the resonance $4Q_x = 25$ (see Ref. [6, 7]), and later in the SIS18 at GSI for the resonance $3Q_x = 13$ (see Ref. [8]).

The mechanism leading to emittance growth and beam loss is explained in terms of instantaneous stable islands in the two-dimensional phase space and their crossing the particle orbits because of the combined effect of space charge and synchrotron motion [9]. The one dimensional resonances allow to discuss the dynamics in one plane.

The key features understood from past studies are summarized in the following qualitative points:

- a) The space charge detuning determines the position of the fixed-points generated by the 1D resonance, which is approximately given by the condition

$$n[Q_{x0} + \Delta Q_x(X)] = N, \quad (1)$$

where here X is the amplitude of the resonant particle, and $\Delta Q_x(X)$ is the incoherent amplitude dependent space charge detuning. For $X = 0$ the quantity $\Delta Q_x(0)$ corresponds to the usual incoherent tune-shift.

- b) The strength of the resonance determines the tune of particles around the fixed-points, and consequently how large is the island. The island size has folded-in also the detuning created by space charge: stronger gradients in the amplitude dependent detuning leads to smaller islands.
- c) The synchrotron tune determines how fast is the resonance crossing. A figure of merit on how fast the resonance crossing is, is given by the parameter T obtained as the ratio between the speed of migration of the fixed-points to the maximum speed of rotation of the particle in the island. If this ratio is small ($T \ll 1$) it means that the motion is adiabatic, and the particles remain locked to the island (trapping); If instead $T > 1$ then a single resonance crossing produces a “kick” to the particle invariant (scattering).

The standard accelerators settings bring the dynamics mainly to scattering processes, which are highly dependent from the strength of the resonance, space charge tune-shift, distance from the resonance, and synchrotron tune.

THE DIFFICULTY OF THE TWO DIMENSIONAL RESONANCES

For a two dimensional resonance as $n_x Q_x + n_y Q_y = N$, the dynamics are coupled. That means that a two dimensional analysis of the Poincaré section of the coordinates x, x' does not provides the proper understanding. The major difficulty

is in understanding how the space charge modify the tori embedded in the four dimensional phase space. Usually the tune-spread is not the same in horizontal and vertical planes, hence it is particularly difficult to conclude on the process of halo formation, and on its extension in the $x - y$ plane. The meaning of trapping/scattering is also not straightforward to define.

MEASUREMENTS ON THE 3RD ORDER COUPLED RESONANCE

Recently the LIU project at CERN [10] has engaged in studies to explore space charge effects [11], and in investigating the long term storage for high intensity bunches as well. In the framework of the CERN-GSI collaboration, studies on the effect of space charge on the resonance $Q_x + 2Q_y = 19$, have been carried out in the CERN-PS in 2012. We present here a short summary of the full experiment analysis. A more comprehensive presentation of the experimental results and discussion is part of a future publication in Ref. [12].

In the experiment, in a resonance-free region of the tune diagram the third order resonance $Q_x + 2Q_y = 19$ was excited with two nearby sextupoles of strength $K_2 \approx 0.015 \text{ m}^{-2}$. The experimental campaign used a beam with 55×10^{10} protons per bunch, which produced an incoherent space charge tune-shift of $\Delta Q_x \approx -0.05$, $\Delta Q_y \approx -0.07$. The beam was stored at the energy of 2 GeV for 1.1 seconds corresponding to $\sim 0.5 \times 10^6$ turns. During this time, the synchrotron tune $Q_s \sim 8.57 \times 10^{-4}$ induces ~ 1700 possible resonance crossings, and their effect on the beam was assessed by measuring the beam profiles at the beginning and at the end of the storage time.

The measurements were repeated for several machine tunes so to explore the dependence of the effects on the distance from the resonance. The comparison of initial and final beam profiles revealed an unexpected beam response to the distance from the resonance. When the space charge tune-spread overlaps the third order resonance and the machine tune is close to the resonance without beam loss, the beam profiles evolves differently in the transverse planes: in the horizontal plane the beam exhibits core growth, whereas in the other plane a large halo is formed. This is shown in Fig. 1a,b for the tunes $Q_{x0} = 6.104$, $Q_{y0} = 6.476$. The x/y asymmetry of the beam profile is quite evident and shows that a new and more complex dynamics is driving the beam halo formation. In the picture are also shown the profiles from computer simulation as obtained from MADX, and MICROMAP (see Ref. [13] for a general code benchmarking discussion). Figure 1c shows the overall beam response in the experiment. The profiles in Fig. 1a,b correspond to the largest emittance growth.

ANALYSIS WITH DETUNING

The explanation of the halo vs. core finding can be approached from a detuning analysis. The theory of the resonances (see Ref. [14, 15]) shows that the distance from the third order resonance is $\Delta_{r0} = Q_{x0} + 2Q_{y0} - 19$ so that

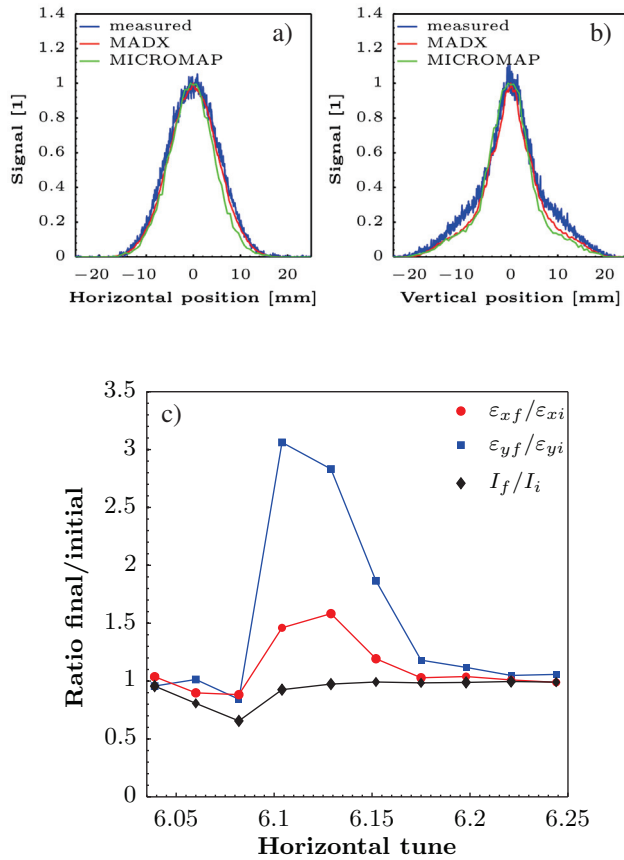


Figure 1: Part a, and b: horizontal and vertical beam profiles after 1.1 second storage of the beam in the CERN-PS. The asymmetry of the beam response is evident. In part c is shown the full beam response to all working points investigated.

when $\Delta_{r0} = 0$ the machine tunes sit on the resonance. This definition valid for the machine tunes can be extended to any arbitrary particle as $\Delta_r = Q_x + 2Q_y - 19$, where now the tunes Q_x, Q_y are the effective tunes experienced by a test particle, which is affected by space charge, chromaticity, and any other effects.

For the case of pure space charge, these tunes are depending on the particle amplitudes X, Y . The amplitude dependent detuning $\Delta Q_{sc,x}(X, Y), \Delta Q_{sc,y}(X, Y)$ is folded in the single particle tune as $Q_x = Q_{x0} + \Delta Q_{sc,x}(X, Y)$, and $Q_y = Q_{y0} + \Delta Q_{sc,y}(X, Y)$, so that

$$\Delta_r = \Delta_{r0} + \Delta Q_{sc,x}(X, Y) + 2\Delta Q_{sc,y}(X, Y). \quad (2)$$

This relation allows for an approximate finding of the amplitudes X, Y of resonant particles. Given the machine tunes Q_{x0}, Q_{y0} we find Δ_{r0} , and the resonant transverse amplitudes X, Y which satisfy the equation $\Delta_r = 0$. More in general Eq. (2) shows that Δ_r is dependent on X, Y , and can be regarded as a “resonance detuning” that incorporates the coupled character of the resonance $Q_x + 2Q_y = 19$ and space charge.

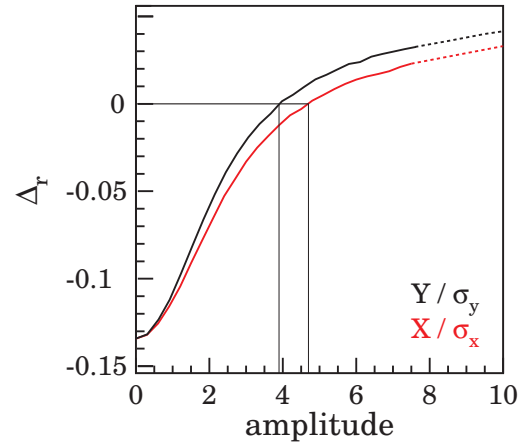


Figure 2: Resonance detuning Δ_r as function of the particle amplitude.

In Fig. 2 the two curves show the dependence of Δ_r for two types of particle amplitudes. The red curve is obtained for amplitudes type $(X, 0)$, while the black curve is obtained for amplitudes $(0, Y)$. The horizontal line of height $\Delta_r = 0$ intercepts the two curves at the resonant amplitudes, which in our case are $X \sim 5\sigma_x$ for the red curve, and $Y \sim 4\sigma_y$ for the black curve.

From the periodic resonance crossing induced by space charge we expect that particle diffusion does not exceed the outer position of the “resonant particles”, which is $X \sim 5\sigma_x$, and $Y \sim 4\sigma_y$. However, a comparison with a multi-particle simulation in absence of chromaticity, shows that no halo with amplitude $X \sim 5\sigma_x$ is found.

By including into Eq. (2) the effect of the chromaticity we investigate the role of the chromaticity on the resonant amplitudes. For example, for particles with maximum $\delta p/p = 2.4 \times 10^{-3}$ we can construct an equivalent graphic of Fig. 2, and search for the resonant particles at largest amplitudes (condition $\Delta_r = 0$). We find that the halo predicted by this analysis is $X > 9\sigma_x$, and $Y \sim 9\sigma_y$. Once more, this result contradicts the experimental findings, in which the halo is found at $Y \approx 5.5\sigma_y \approx 20$ mm.

INTERPRETATION WITH THE FIXED-LINES

The previous analysis based on the detuning ignores the resonant process itself, which clearly is included in the beam profiles observed and retrieved from simulations in Fig. 1. In the absence of space charge, a particle satisfying the resonance condition $\Delta_{r0} = 0$ has dynamics locked to the resonance. Contrary to the 1D resonances, the 2D resonance makes the particle orbit at the Poincaré section to be bounded to a one dimensional closed curve extending in the full 4D phase space. This curve, in analogy to the fixed-points for one dimensional resonances, is a fix-line [15–17].

The analytic form of these closed lines is parameterized as

$$x = \sqrt{\beta_x a_x} \cos(-2t - \alpha + \pi M), y = \sqrt{\beta_y a_y} \cos(t). \quad (3)$$

The coordinates x', y' are readily derived by differentiation. The fixed-line emittances a_x, a_y are determined by the distance to the resonance Δ_{r0} . β_x, β_y are the beta functions at the Poincaré section location. The variable t parameterizes this one dimensional curve. The coefficient M is 0, or 1 according to the condition of existence of the fixed-line. In Fig. 3 we show an example of the projections of one fixed-line plotted in normalized coordinates. The $x - y$ projection has a distinct “8” shape. The $x' - y'$ projection has instead a “C” shape. The dependence of α in Eq. (3) makes the shape “C” and the shape “8” exchangeable according to the location of the Poincaré section: the parameter α is the phase of the driving term of the third order resonance, and it depends on the difference of phase advance between the location of the sextupoles used to excite the resonance with respect to the observation point along the machine (the flying wire position).

The interplay of the resonant dynamics with the space charge is the key issue, and is here presented with a numerical study. The role of the fixed-lines in the bunched beam is

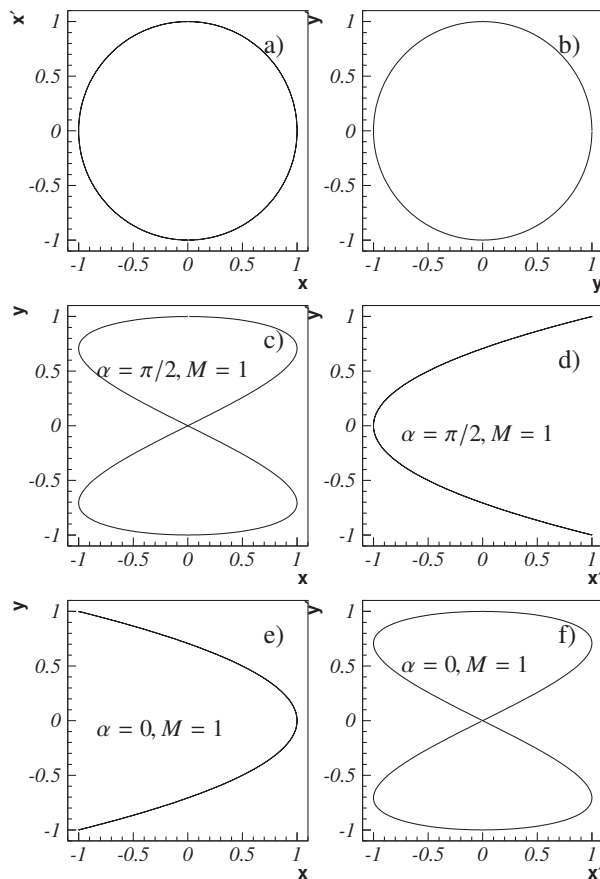


Figure 3: Fixed-line projections in normalized coordinates. The parameters in Eq. (3) are indicated in each picture. Note that the topology of the $x - y$ projection of a fixed-line depends substantially on the angle α .

investigated by freezing artificially the longitudinal motion in the simulation modeling the experimental beam profiles of Fig. 1, and by constructing a tune footprint of a set of test particles. The resonant particles are easily identified using an FFT method. In fact, the main peak of the FFT spectrum yields the nonlinear tunes Q_x, Q_y of the particles satisfying $Q_x + 2Q_y - 19 = 0$. We then plot the $x - y$ projection of the resonant orbits and compare it with the $x - y$ projections in Fig. 3 searching for indications of a fixed-line dynamics. In part a of Fig. 4 we show two resonant orbits for test particles located at $z/\sigma_z = 0$. The topology of the orbit projection leaves no doubt that we see two particles locked to two distinct fixed-lines having the “8” shape in $x - y$ projection. The asymmetric form of the orbits is remarkable although the resonant particle is not sitting exactly on the fixed-line (we see more the projection of a resonant tori). This result simply shows that the presence of the beam space charge detuning does not destroy the dynamics that creates the fixed-lines. By repeating the same analysis for particles at $z/\sigma_z = 1.5$ we can visualize the resonant orbits at a location of the bunch with smaller transverse space charge. These resonant orbits are shown in part b of Fig. 4. Even in this case we clearly distinguish in the resonant orbits the pattern of fixed-lines. The aspect ratio is now different, and the extension of the orbits is smaller.

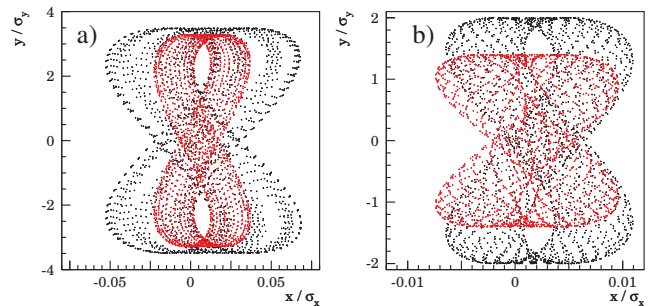


Figure 4: Part a). $x - y$ projection of the two largest resonant orbits at $z/\sigma_z = 0$; Part b). The two largest resonant orbits now at $z/\sigma_z = 1.5$.

The extension of the “frozen” fixed-lines along the bunch is consistent with the studies on one dimensional resonances. In Ref. [9] it is shown that the frozen transverse islands have the maximum size and their fixed-points have maximum amplitudes at longitudinal positions $z/\sigma_z = 0$. For other longitudinal positions within the bunch the fixed-points are found at smaller amplitudes. Eventually at locations far enough from the bunch center, the fixed-points merge to the transverse origin and disappear. This pattern is at the base of the periodic resonance crossing mechanism. Figure 4a,b convey the same information as they show that instantaneous fixed-lines have amplitude function of the longitudinal particle coordinate z . This pattern which exhibits the largest fixed-lines at $z/\sigma_z = 0$, with amplitude decreasing for increasing the longitudinal amplitude, will create phenomena

of periodic crossing of the fixed-lines. This can be seen in Fig. 5 where the evolution of the emittance of one test particle is shown during one synchrotron oscillation. The test particle is one of those used in the simulation for obtaining the profiles a), b) of Fig. 1, where the effect of chromaticity is included. The scattering of the single particle emittance is clearly visible with 4 kicks per synchrotron oscillation.

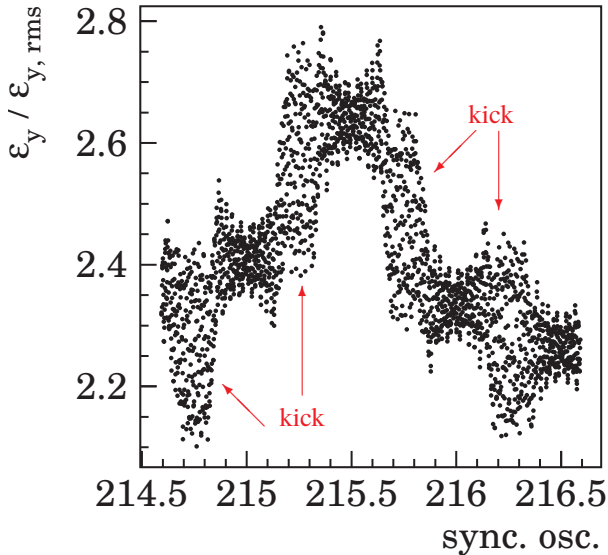


Figure 5: Emittance of one test particle during storage. The picture reveals the 4 kicks exerted by the fixed-lines during one synchrotron oscillation.

CONCLUSION AND OUTLOOK

We have here shortly summarized the main findings of the PS experiment performed in 2012. We find in simulations the evidence that the dynamics creating the halo is controlled by the fixed-lines. We find that the fixed-lines amplitude is a function of the instantaneous space charge tune-spread, which depends on the particle longitudinal position within the bunch. This induces a phenomena of periodic crossing of the fixed-lines with the particle orbit. Scattering phenomena are found in the simulation as a clear trace of this fundamental mechanism. We conclude that the x/y asymmetry of the measured beam response (Fig. 1 a,b) is the result of the asymmetric shape of the instantaneous fixed-lines (Fig. 4) provided the effect of chromaticity is included.

It remains open and is not discussed in this proceeding the influence of the many fixed-lines on the particle motion, and the explanation of why the halo in the experiment extends only up to $5.5\sigma_y$, although simulations clearly show the existence of many fixed-lines which extends on a larger surface, reaching up to $9\sigma_y$, when the effect of the chromaticity is included. The understanding of this mechanism is also of relevance on the issue of the resonance compensation [18]. The discussion of all these aspects as well as of the open question here presented is left to future studies.

ACKNOWLEDGMENT

The research leading to these results has received funding from the European Commission under the FP7 Research Infrastructures project EuCARD-2, grant agreement no. 312453.

REFERENCES

- [1] O. Kester, P. Spiller, and H. Stoecker, in *Challenges and Goals for Accelerators in the XXI Century*, edited by O. Brüning and S. Myers (World Scientific, Singapore, 2016), p. 611.
- [2] J. Struckmeier, *Phys. Rev. ST Accel. Beams*, **3** 034202, 2000.
- [3] O. Boine-Frankenheim, I. Hofmann, J. Struckmeier, and S. Appel, *Nucl. Instrum. Methods Phys. Res., Sect. A* **770**, 164 (2015).
- [4] I. Hofmann and O. Boine-Frankenheim, *Phys. Rev. ST Accel. Beams* **17**, 124201 (2014).
- [5] Kesting Frederik and Franchetti Giuliano, *Phys. Rev. ST Accel. Beams* **18**, 1142201 (2015).
- [6] G. Franchetti, I. Hofmann, M. Giovannozzi, M. Martini, and E. Métral, *Phys. Rev. ST Accel. Beams* **6**, 124201 (2003).
- [7] E. Métral, G. Franchetti, M. Giovannozzi, I. Hofmann, M. Martini, and R. Steerenberg, *Nucl. Instr. and Meth. A* **561**, (2006), 257-265.
- [8] G. Franchetti, O. Chorniy, I. Hofmann, W. Bayer, F. Becker, P. Forck, T. Giacomini, M. Kirk, T. Mohite, C. Omet, A. Parfenova, and P. Schuett, *Phys. Rev. ST Accel. Beams* **13**, 114203 (2010).
- [9] G. Franchetti and I. Hofmann, *Nucl. Instr. and Meth. A* **561**, (2006), 195-202.
- [10] J. Coupard *et al.*, “LHC Injectors Upgrade, Technical Design Report, Vol. I: Protons”, LIU Technical Design Report (TDR), CERN-ACC-2014-0337.
- [11] V. Forte, E. Benedetto, and M. McAteer, *Phys. Rev. Accel. Beams* **19**, 124202 (2016).
- [12] G. Franchetti, S. Gilardoni, A. Huschauer, F. Schmidt, and R. Wasef, submitted to PRAB.
- [13] H. Bartosik *et al.*, in *Proc. HB2016*, Malmö, Sweden. paper WEAMIX01. p. 357.
- [14] A. Schoch, “Theory of Linear and Non-Linear Perturbations of Betatron Oscillations in Alternating Gradient Synchrotrons”, CERN 57-21 (Proton Synchrotron Division), Section 14 (1958).
- [15] G. Franchetti and F. Schmidt, *Phys. Rev. Lett.* **114**, 234801 (2015).
- [16] G. Franchetti and F. Schmidt, <http://arxiv.org/abs/1504.04389>
- [17] F. Schmidt, “Untersuchungen zur dynamischen Akzeptanz von Protonenbeschleunigern und ihre Begrenzung durch chaotische Bewegung”, PhD thesis, DESY HERA 88-02 (1988).
- [18] G. Franchetti, S. Aumon, F. Kesting, H. Liebermann, C. Omet, D. Ondreka, R. Singh, S. Gilardoni, A. Huschauer, F. Schmidt, and R. Wasef, in *Proc. HB2014*, East Lansing, MI, USA, paper THO1LR03. p. 330.